The Birth of Exoplanets: Alpha Enhancement and the Formation of Planetary Systems

By Ryan Schmitt

Abstract:

The discovery of over 400 exoplanets has facilitated increasing statistical research, especially when considering their formation and chemical abundances. Iron abundance, is used as a proxy for elemental abundance studies in astronomy, and new research suggests a correlation between the iron abundance of the host stars and the existence of exoplanets. While iron abundance of all of the host stars has been explored, very little is known of their other elemental abundances. Studying elements other than iron provides insight into the conditions that lead to a star's birth and the formation of exoplanetary systems. I will present spectroscopic analysis of the photospheric elemental abundances of two particular star systems: HD 89307, which is the most similar exoplanetary host star to the Sun, and Gliese 581, which has two planets that reside within the habitable zone. Using high-resolution echelle spectra from the ELODIE archive at Observatoire de Haute-Provence, I measured iron abundances consistent with modern empirical values for both of the chosen stars. I explored other elements, and it was apparent that HD 89307 has higher than solar abundances. I analyzed the elemental abundances of Gliese 581, which has a lower metallicity compared to that of the Sun, and calculated higher elemental abundances for cobalt, nickel, and silicon. Finally, I compare the specific abundances calculated to the abundances of the Sun and investigate the likelihood of a trend.

Introduction:

In order to begin this analysis, it is important to recognize an interesting trademark in exoplanets, namely the fact that there is a correlation between metallicity of the host star and the existence of exoplanets. Metallicity is the abundance of all elements heavier than Hydrogen and Helium. To get a proxy for the total metallicity, astronomers tend to use the abundance of iron to hydrogen (hydrogen being the most abundant element in the universe). Mathematically, the ratio is defined as

$$[\frac{Fe}{H}] = log(\frac{N_{Fe}}{N_H})_{star} - log(\frac{N_{Fe}}{N_H})_{sun},$$

where [Fe/H] is the ratio of the logarithm of iron to hydrogen for a particular star compared to the sun. N_{Fe} and N_H are the number of atoms for the respective element per unit volume. By definition, the iron abundance for the sun is [Fe/H]=0.00.

Through spectroscopic analysis, astronomers have discovered that stars that have higher metallicities are most likely to harbor planets (Gonzalez, 2003). Figure 1 is a graph showing the percentage of stars with planets versus iron abundance of the star. This was part of survey that studied 1330 FGKM class stars with varying iron

abundances and the exoplanetary systems they discovered. The obvious pattern suggests that a star must have adequate metallicity in order to have planets present within the system (Marcy, et al., 2005).

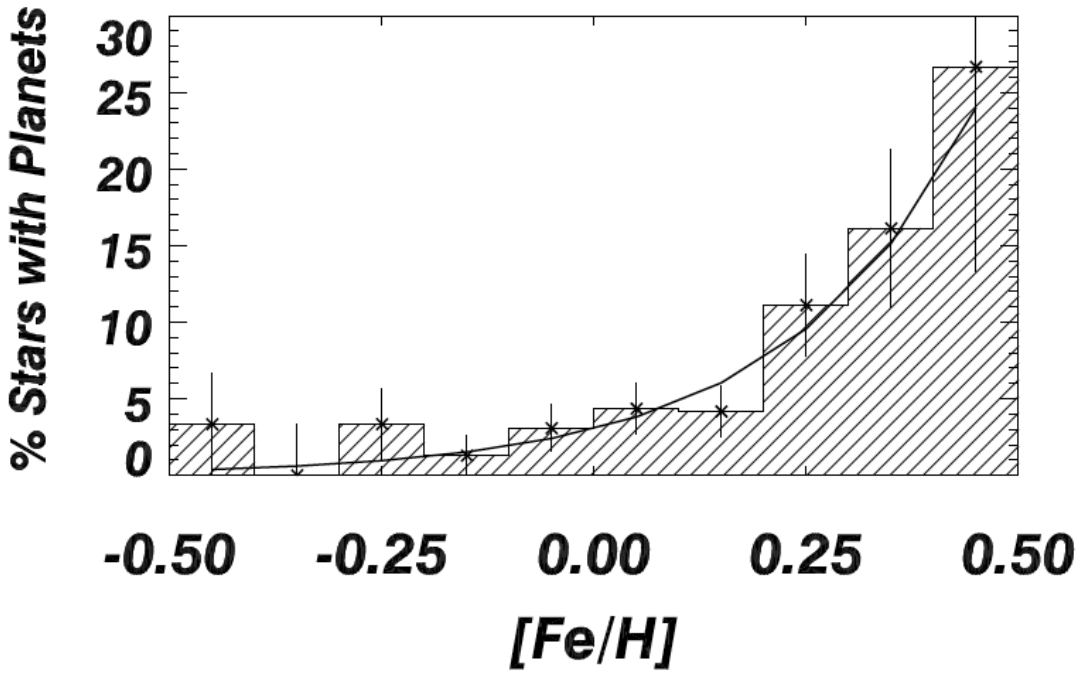

Figure 1: The correlation of iron abundance and the percentage of stars that have planets, with higher metallicity stars being more likely to harbor planets. This was part of an ongoing survey of 1330 FGKM stars (Marcy, et al., 2005).

While planet hunters have done an excellent job of bringing to light the amazing discovery of planets outside our solar system, very little research has been done on the elemental abundances beyond iron, and that is the main focus of this research project. In order to decide which elements to study, it is important to look at stellar evolution. Supernova explosions provide the catalyst needed to fuse heavier elements, and there are two distinct types of supernova, each of which are responsible for producing distinct elemental abundances inherent to the type of supernova.

There is a Type Ia supernova, which is due to a white dwarf accreting matter off a companion star, which eventually leads to a greater mass than the Chandesekar limit (defined as 1.4 M_{sun}). Once the white dwarf breaks this limit, the reaction that results is a supernova explosion. Through the resulting fusion, the iron peak elements (V, Cr, Mn, Fe, Co, Ni) are produced. They are known as iron peak elements because elements can be produced through stellar nucleosynthesis up to iron, and to fuse elements beyond this peak(A>56), supernova nucleosynthesis is required. A plot of binding energy per nucleon versus nucleon number shows this peak visually, and an example is given in figure 2.

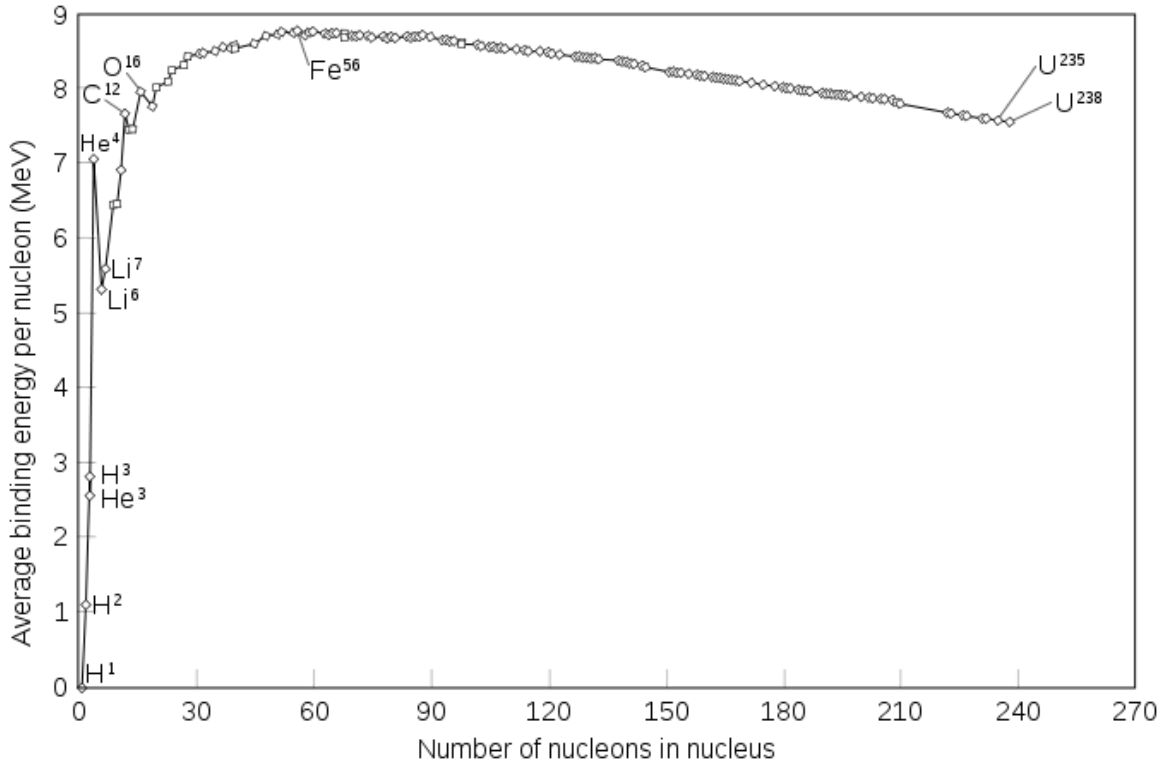

Figure 2: Binding energy per nucleon versus the number of nucleon in a nucleus for a given element. Iron peak elements are called such because they have the highest average binding energy per nucleon.

Type Ia supernovae are not the only supernovae that produce heavier elements. The triple alpha process and alpha elements, C, N, O, Ne, Mg, Si, S, Ar, Ca and Ti, are produced due to late stellar evolution of a single star and the resulting type II supernova (elements that are heavier than iron, A>56, are produced due to the r-process from the resulting supernova shockwave). Alpha elements are called such because they are integer multiples of the mass of the helium nucleus (also known as the "alpha particle"). To better understand how elements are created via these processes, I will show some examples:

1) The Triple Alpha Process

$$^{4}_{2}He + ^{4}_{2}He \rightarrow ^{8}_{4}Be$$

$$^{8}_{4}Be + ^{4}_{2}He \rightarrow ^{12}_{6}C + \gamma$$

The first step consists of two helium "alpha" particles that produce an unstable beryllium nucleus. This unstable nucleus must be struck by another alpha particle, otherwise it will decay back down into two separate helium nuclei. Once enough carbon is produced, alpha elements can then be formed.

2) Alpha Capture

$$^{12}_{6}C + ^{4}_{2}He \rightarrow ^{16}_{8}O + \gamma$$

$$^{16}_{8}O + ^{4}_{2}He \rightarrow ^{20}_{10}Ne + \gamma$$

With ample carbon, alpha particles will then join with the carbon to produce stable oxygen. This process continues until neon, magnesium, silicon and sulfur are produced.

While some of these elements can fuse within a star, due to the process of stellar nucleosynthesis, the heavier alpha elements are formed due to a Type II supernova. A Type II supernova is well known as the dramatic explosion of a single massive star. After burning all possible silicon into iron, the core can no longer produce the radiative pressure necessary to keep the gravitational pressure in equilibrium, and the core collapses. With all of the mass rushing to the core, a massive shock wave is created, that produces a very luminous event as well as sending a huge flux of neutrons into space. These neutrons fuse with other nuclei as the shockwave interacts with interstellar material, producing the heavier r-process (A>56) elements.

New stars are formed from the ejected remains of old stars, hence the term 2nd Generation stars. These stars then have the capability of forming planetary systems. In order to understand how these systems may be formed and the elemental abundances that can be observed, I looked at solar system abundances. Photospheric abundances of the Sun have been obtained spectroscopically by astronomers, while solar system abundances include abundances of the atmospheres of gas giants, the composition of rocky planets, and meteoritic findings, namely CI Chondrites. CI Chondrites are a classification of Carbonaceus Chondrites, which are meteorites that most closely resemble solar composition. By comparing the elemental abundance of the Sun's photosphere with the abundance of CI Chondrites, it is interesting to note that for most elements, the abundance is the same for both (Lodders, 2003, Hartmann, 2005).

In astronomy, the logarithmic astronomical scale is often utilized when describing elemental abundances other than iron, and is defined as

$$A(El) = log(\frac{N_{El}}{N_H})_{star} + 12$$

where **A(El)** and **N(El)** are the abundance and number of atoms per unit volume, respectively. The abundance of hydrogen is defined as A(H) =12, because there are 12 orders of magnitude difference between the number of hydrogen atoms, the most

abundant element in the solar system, and uranium which is the least abundant (Lodders, 2003).

In order to visualize the range of abundances for the solar system, Figure 3 shows a plot of log astronomical scale versus atomic number, Z. Notice the general peaks around the alpha process elements, and the iron peak elements.

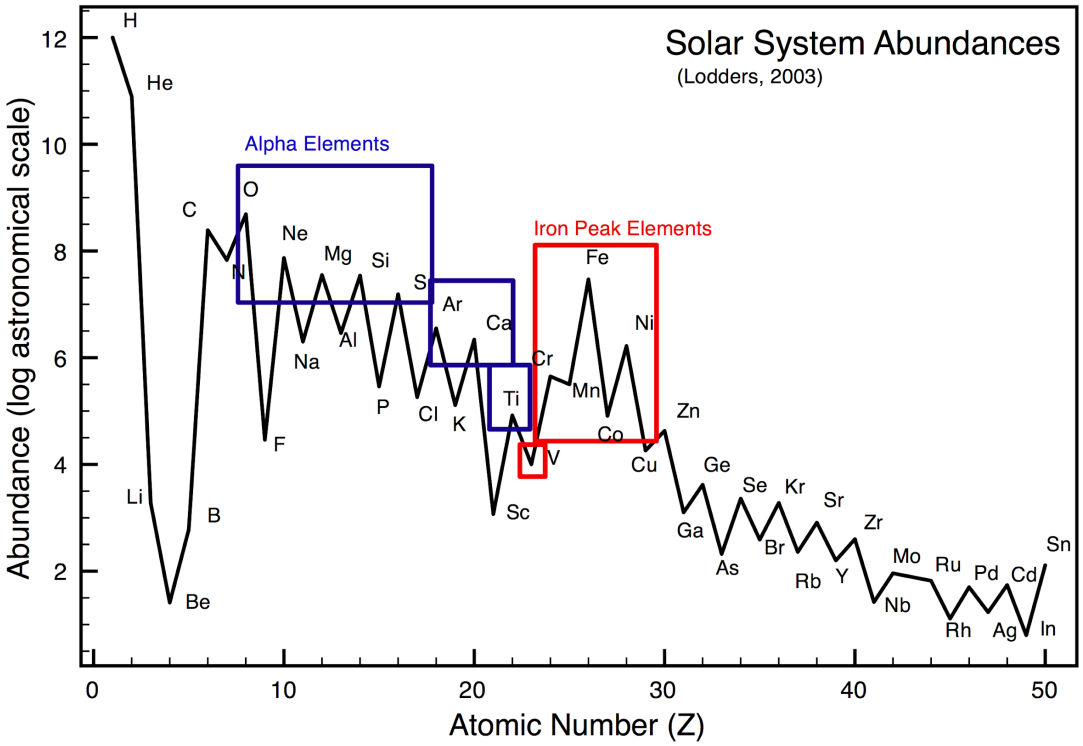

Figure 3: Elemental abundance versus atomic number Z, for all elements ranging from hydrogen to uranium (Lodders, 2003). The alpha elements and the iron peak elements are the most abundant elements in the solar system, and comparing these abundances of exoplanetary host stars is the purpose of this study.

Considering what could be learned from photospheric elemental abundances and how they relate to extrasolar system abundances, there were 4 major parameters for choosing elements:

1) To confirm previous measurements of iron abundance of the host stars, I need to look at Fe, and other iron peak elements, due to type Ia supernovae.
2) In order to understand alpha elemental abundances, especially when compared to iron abundance findings, there must be a selection of alpha elements that are attainable through spectroscopic research.

3) To make ideal comparisons to CI Chondrite abundances, elements are needed that have equal or near equal photospheric abundances to Chondrite abundances.
4) To see if there is significant biological elemental abundances, for possible astrobiological applications.

I decided upon the CNO elements, carbon(C), nitrogen(N), oxygen(O); the alpha elements, magnesium(Mg), silicon(Si), sulfur(S), calcium(Ca); the iron peak elements, iron(Fe), cobalt(Co), nickel(Ni); and finally sodium(Na), Aluminum(Al) and potassium(K), for their biological significance. With a firm idea of what elements I would be studying, I then found the exact wavelengths where these absorption lines appear.

To discover the exact wavelengths that these atoms absorbed light, I referred to the NIST: Atomic Spectra Database, which provides all information necessary for measurement of absorption lines at particular wavelengths and other important values such as energies, atomic mass, and possible transitions. The wavelength range of interest is in the visible spectrum, and for the ELODIE archive, this is between 4000 to 6800 Angstroms.

There will be two star systems that will be the focus for this investigation, namely HD 89307 and Gliese 581. The reasoning for these choices resides in the fact that HD 89307 works as a good base considering it so closely resembles the sun in mass, radius, temperature and metallicity. Gliese 581 was chosen because it not only harbors planets with similar masses to our own rocky planets, but two of these planets reside within the range known as the habitable zone, which is defined as the range of distances a planet's orbit can reside and be in a range of temperatures where liquid water could exist. Figure 4 is a list of stellar properties for these two stars.

Stellar Properties	**HD 89307 (*)**	**Gliese 581 (⊗)**
Distance from the Sun (pc)	30.91	6.26
Mass (Msun)	1.00	.31
Radius (Rsun)	1.07	.38
Spectral Type	G0V	M3
Effective Temperature (K)	5950	3480
Luminosity (Lsun)	1.3	.013
Log g (surface gravity)	4.414	4.92
Iron Abundance (compared to solar)	-0.14±.04	-.33±.12

Figure 4: A Table showing various stellar properties of the two stars in question. These values (except for distance) are important for abundance analysis. (*Fischer, et al., 2009, ⊗Bean, et al., 2006)

In order to study the selected host stars, the above information is used as a basis for confirming iron abundance, as well as picking the correct stellar model with the proper effective temperature, mass, and surface gravity. Once iron abundance measurements can be confirmed as being within the range of previous measurements, then the calculation of other elemental abundances can begin.

Method:

In order to determine photospheric elemental abundances, the first necessary component are the spectra of the star, which is composed of a symphony of absorption and emission lines, which correspond to differing energy levels of a particular atom or molecule. For this investigation, spectra are obtained from the ELODIE archive, which is a high-resolution visible light echelle spectrograph archive for the Observatoire de Haute-Provence in France. The main reasons for choosing this particular archive is the ease of use, the fact that telluric lines (absorption lines due to the earth's atmosphere) were already subtracted from the spectra, and since the spectrograph is no longer in operation, most of the spectra are made available to the public. The spectra had to be properly calibrated, due to the slight redshift of the stars in question.

By measuring the equivalent width of a line, one can determine a relative abundance. Equivalent width is given as

$$W(\lambda) = \int \frac{I_c(\lambda) - I_\lambda(\lambda)}{I_c(\lambda)} d\lambda ,$$

with $I_c(\lambda)$ and $I_\lambda(\lambda)$ being the intensity as a function of wavelength of the continuum and intensity of absorption line at a particular wavelength, respectively. It can also be thought of as the area of the rectangle from the continuum to zero that is equivalent to the area of the absorption line. On a plot it would look like the example given below, where W_1 and W_2 are two equivalent widths for the given sodium doublet. This plot is an example of the observed ELODIE spectra, with the model spectra used to calculate abundances. The intensity has been normalized, and the wavelength is in Angstroms.

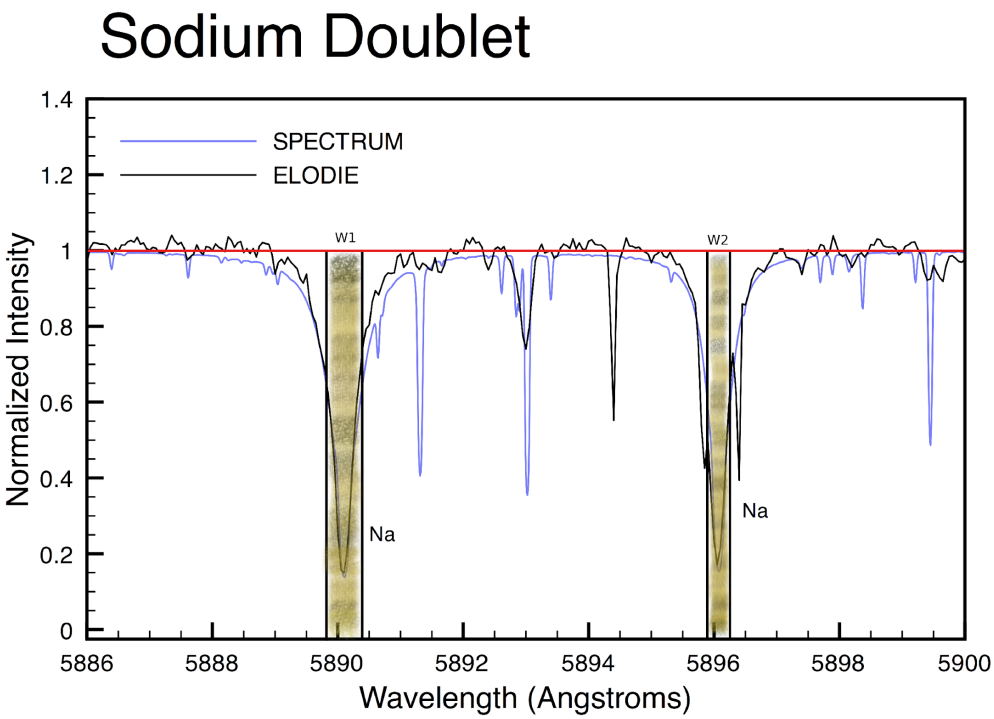

Figure 5: An example spectrum showing the equivalent widths of the sodium doublet. The rectangles represent the equivalent area of the absorption line base of the continuum.

There is a distinct relationship between the equivalent width of a line, and the number of atoms present for a volume in question. A Unix GUI program written by Dr. Peter Draper, called SPLAT-VO, was used for analyzing spectra. An example of the output of this program is given in Figure 6. Within the program it is possible to fit a continuum polynomial equation of various degrees, and fit various profiles (such as Gaussian, Lorentzian, and Voight), to a particular line. Gaussian profiles are utilized in this research, in order to come up with equivalent widths for abundance calculations. While Lorentzian profiles are the best fit for absorption lines, they are mathematically complex. Gaussian profiles are used because they are easy to deal with mathematically and they are good fits for the core of the absorption lines. In any case, there was not much of a difference in abundance values between using Lorentzian and Gaussian profiles.

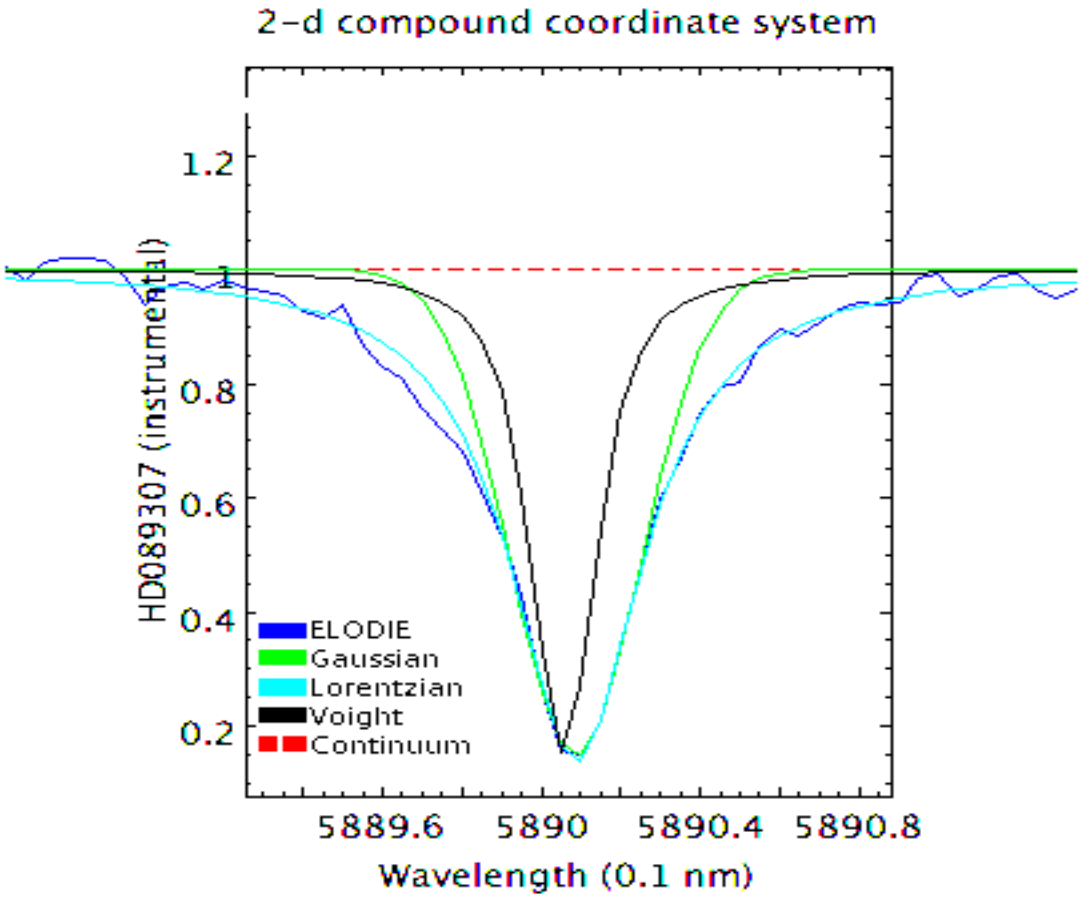

Figure 6: An example output from SPLAT-VO, showing various profiles calculated for a sodium absorption line. The data is from the ELODIE archive. Gaussian profiles are utilized for the equivalent width measurements.

The Gaussian function utilized by SPLAT-VO is of the form

$$I(\lambda) = Ae^{\left(-\frac{1}{2}\left(\frac{\lambda - c}{\sigma}\right)^2\right)},$$

where **I(λ)** is the intensity at a particular wavelength, **A** the Gaussian peak amplitude, **c** the center position of the Gaussian peak, and **σ** is the width. The equivalent width of a Gaussian fit is

$$W(\lambda) = A\sigma\sqrt{2\pi}.$$

SPLAT-VO outputs **A, c,** and **σ,** as well as the errors associated with the calculations, and these will be utilized for abundance calculations.

Once the equivalent width of over 450 absorption lines is measured for each star, the values from SPLAT-VO are inputted into a C++ program written by Dr. Richard Gray called SPECTRUM, which not only plotted model spectra, but could also perform abundance calculations with two auxiliary programs called BLACKWEL and ABUNDANCE. SPECTRUM uses the ATLAS9 models developed by Dr. Robert Kurucz (Kurucz, 2008). These models assume Local Thermodynamic Equilibrium (LTE), which is a local environment of photons and particles confined to a certain volume with a constant temperature. While the assumption that a star in thermodynamic equilibrium is not 100% correct, such an assumption can be utilized to determine relative abundances.

Models are utilized that fit the given effective temperature, metallicity and the surface gravity of the stars in question. The models input these values, as well as the values, mass depth, temperature, gas pressure, for each of the 64 layers of the stars atmosphere. Using SPECTRUM, and inputting the models which best represented the two stars, their respective spectra are calculated. The output spectrum plots normalized intensity versus wavelength, which can be seen compared with an observational spectrum. While the model spectra for HD 89307 gives almost exact equivalent widths to those observed (see Figure 7), the model spectra for Gliese 581 does not seem to fit the observations very well, as seen in the example spectra given in Figure 8. There is some mention by Dr. Richard Gray of the difficulty presented with modeling the spectra of M-class stars (e.g. Gliese 581), but the model could still provide reasonable abundance calculations.

HD 89307:

A)

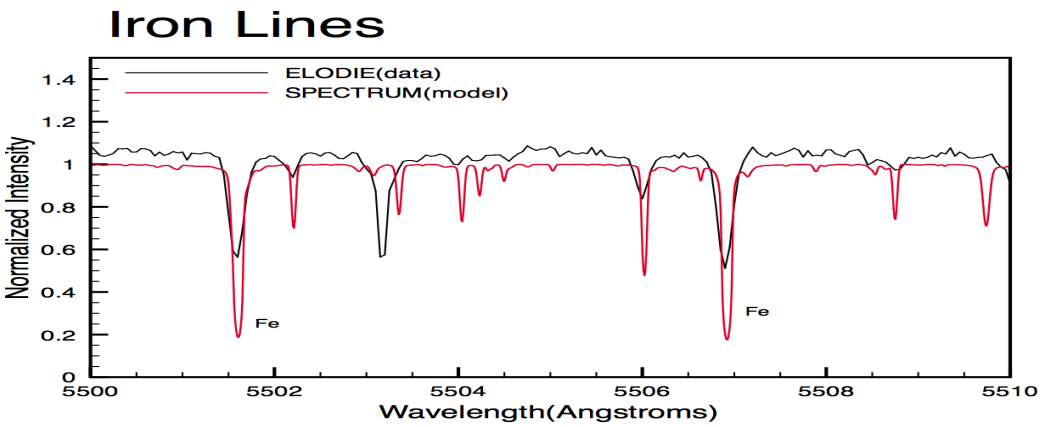
Iron Lines
ELODIE(data)
SPECTRUM(model)
Normalized Intensity
Fe
Fe
Wavelength(Angstroms)

B)

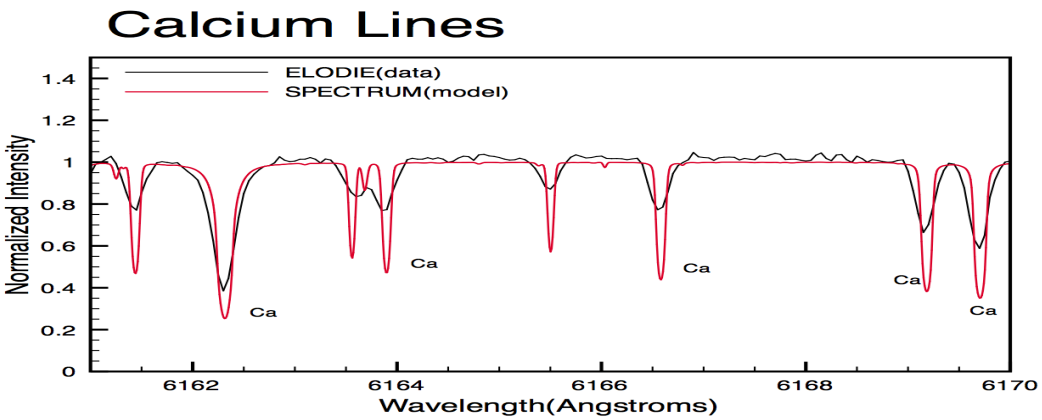
Calcium Lines
ELODIE(data)
SPECTRUM(model)
Normalized Intensity
Ca
Ca
Ca
Ca
Ca
Wavelength(Angstroms)

C)

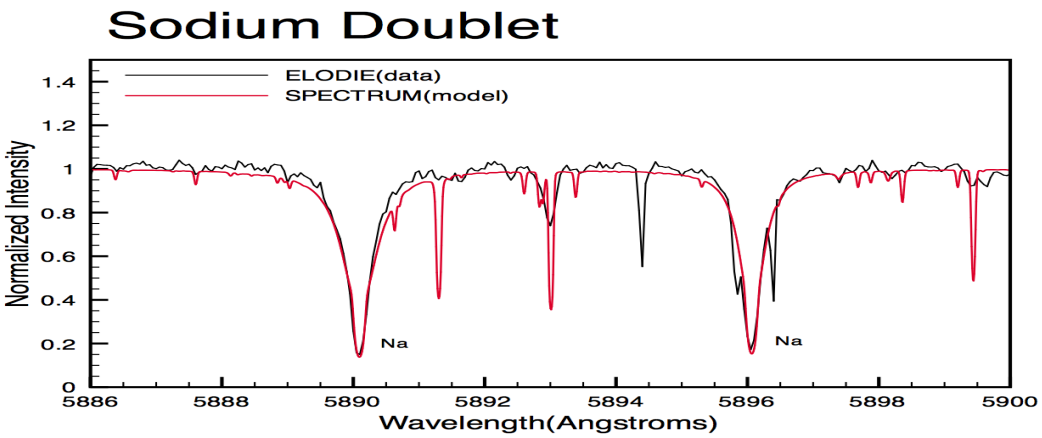
Sodium Doublet
ELODIE(data)
SPECTRUM(model)
Normalized Intensity
Na
Na
Wavelength(Angstroms)

Figure 7(A-C): Three example plots of the model and the observed spectra that show iron, calcium, and sodium lines. The equivalent widths of the model near match that of the observed spectra for HD 89307.

Gliese 581:

A)

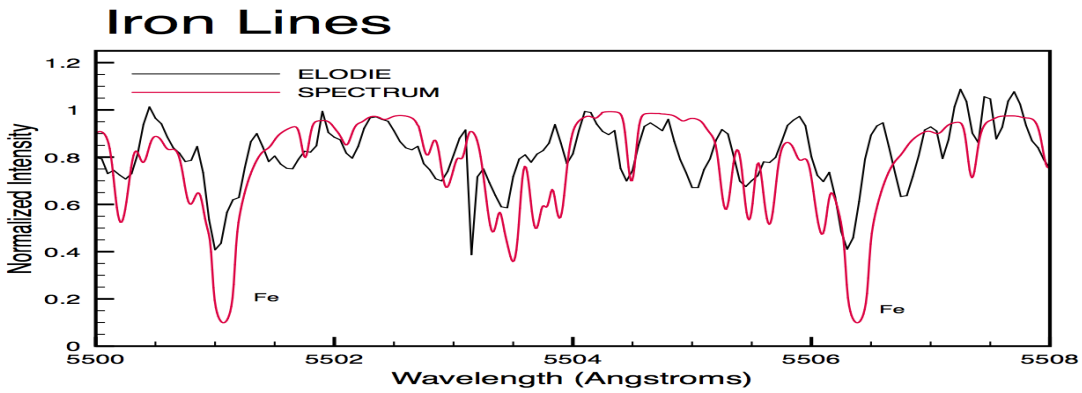

B)

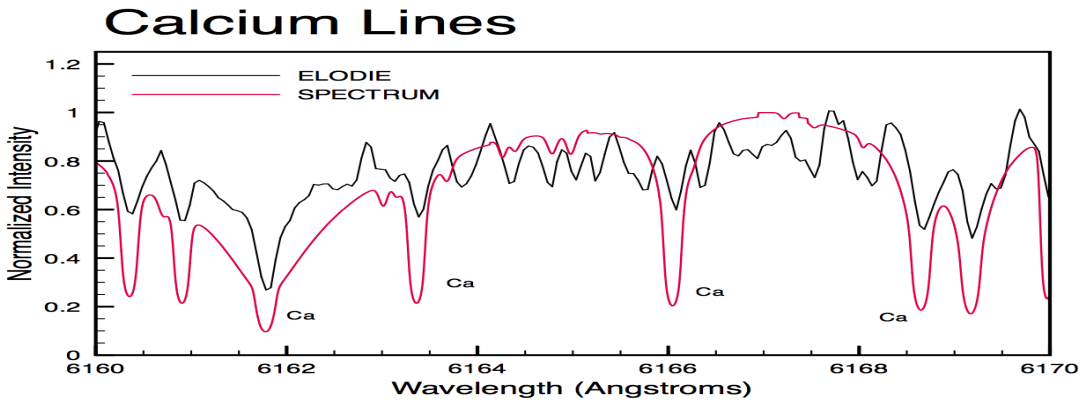

C)

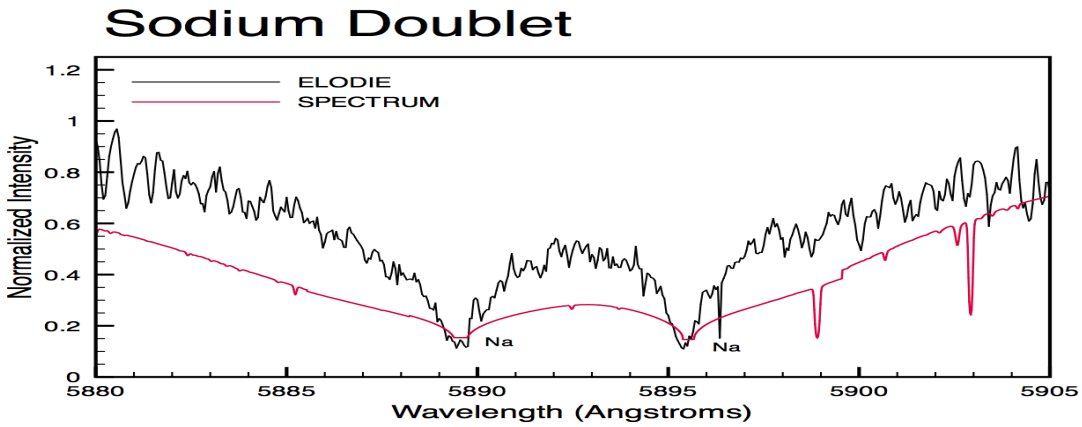

Figure 8(A-C): Model and observational spectra of Gliese 581, showing the same elemental lines as HD89307. The model is a poor fit for the data.

The BLACKWEL program is able to determine the iron abundance versus microturbulent velocity and outputs the values. Microturbulent velocity is the velocity of gas particles over small distances due to convection within a star, and this velocity can cause broadening of spectral lines. The plot of abundance versus microturbulent velocity is called a Blackwell diagram (Blackwell, 1979). Blackwell diagrams are utilized in order to find a range of microturbulent velocities, so that they can then be entered into ABUNDANCE. When looking at a Blackwell diagram (e.g. Figure 9), it is important to notice that each line represents the abundance at a particular wavelength versus microturbulent velocity. By plotting multiple lines corresponding to the particular wavelengths explored, one can see them all intersecting. These intersections, especially larger groupings of lines intersecting at relatively the same place, show where the abundance corresponds with a given microturbulent velocity, and can then be used with the known iron abundance to determine the range of possible microturbulent velocities.

The range of microturbulent velocity is then inputted with the measured observational equivalent widths into the ABUNDANCE program, which outputs the relative abundances for each absorption line. From the varying range of microturbulent velocity, the abundance was not altered significantly. For example, the iron abundance of a particular line for HD 89307 would range from 7.30 to 7.41 (log astronomical scale) given the range of microturbulent velocity, which is between 2 to 3 km/s. Since this was not a major difference, the median (2.5 km/s) of the velocity ranges was inputted into ABUNDANCE.

Results:

HD89307:

The Blackwell diagram for HD 89307 (given in Figure 9) consists of 10 absorption lines of Fe over the entire spectrum, and the results show microturbulent velocities ranging from about 2.4 to 2.9 km/s. The range of microturbulent velocity, along

with the equivalent width measurements, is inputted into ABUNDANCE. The observed mean fit the previous measurement for the iron abundance of HD 89307, which is 7.33±0.03 (Fischer, et. al., 2008). Since HD 89307 is so similar to the Sun, most of the abundances are within close proximity of solar abundances, with calcium, carbon, cobalt, nickel, silicon, sodium, and sulfur being slightly higher than solar values. Elements that seemed to be over abundant were nitrogen and potassium. This may be due to the difficulty of resolving these lines out of the observed spectrum, and with better resolution, perhaps more reliable measurements could be made.

Figure 9 and Figure 10 are detailed plots illustrating the Blackwell diagram and the ABUNDANCE results, respectively, for HD 89307. Notice the circle on the Blackwell diagram point out the major intersections within the given abundance values (from Fischer, et. al., 2008), hence giving an approximation for microturbulent velocity. The ABUNDANCE results (Figure 10) show iron abundance, along with four groups of elements previously mentioned: the CNO elements, the iron peak elements, alpha elements, and biologically significant elements. A solid color line represents the mean of an elemental abundance, with the value of the mean given in the legend.

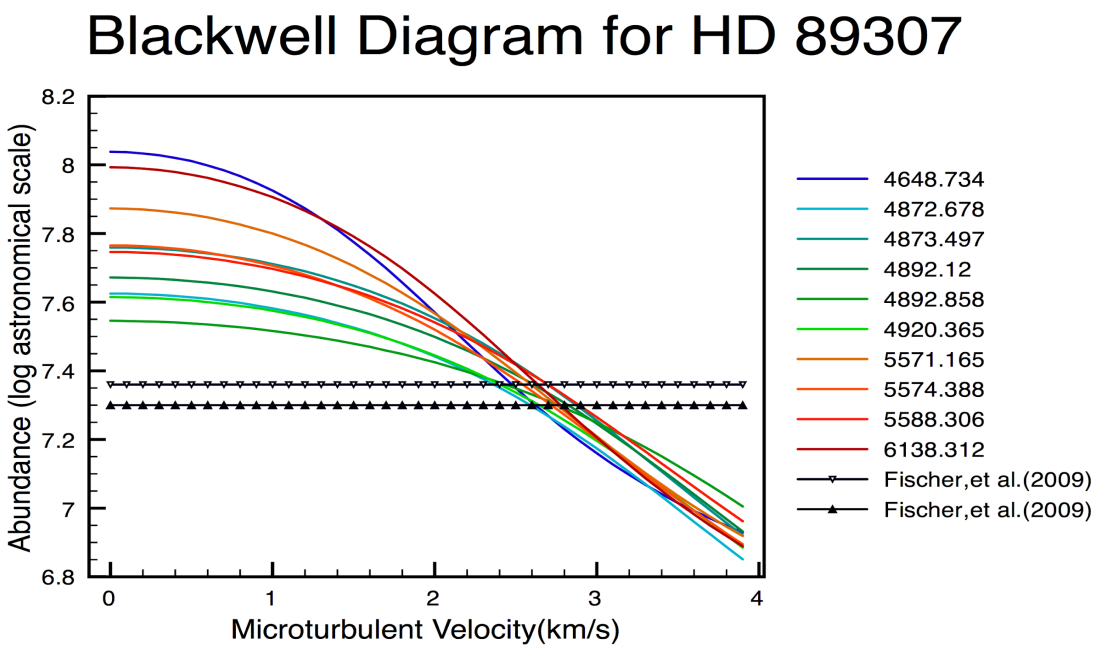

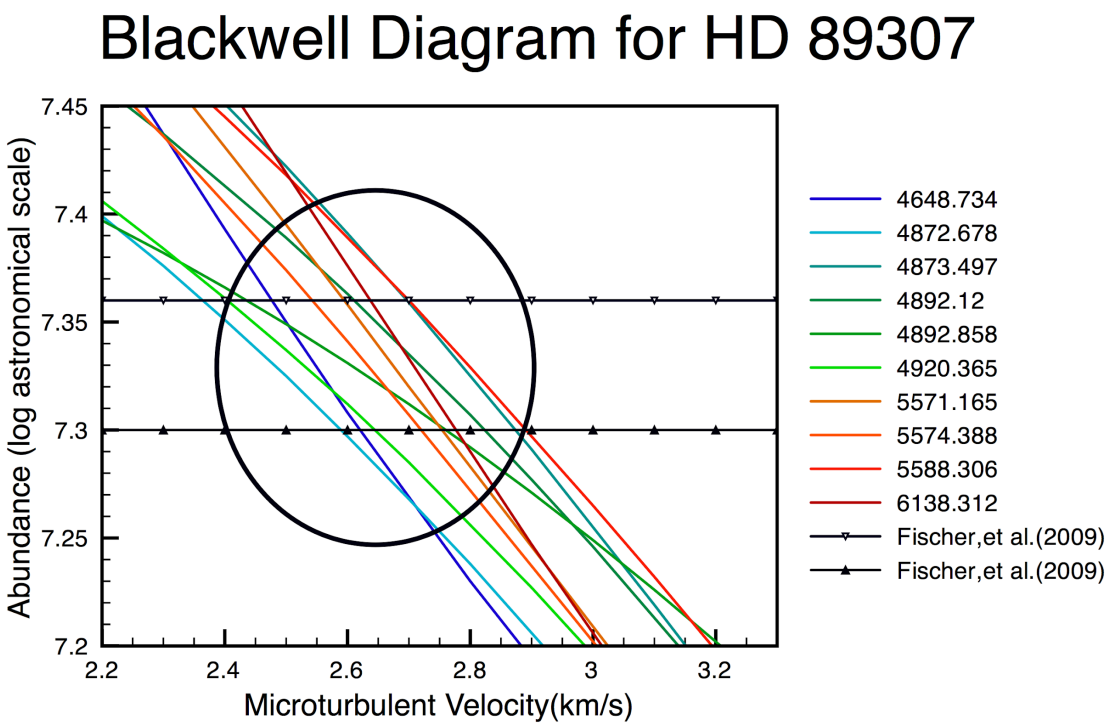

Figure 9: Two plots showing the same Blackwell diagram for 10 Fe absorption lines for HD 89307, the second being a zoomed in cut out. The circle indicates where the majority of intersections happen with in the given value for iron abundance. It shows a microturbulent velocity between 2.40 and 2.90 km/s.

A)

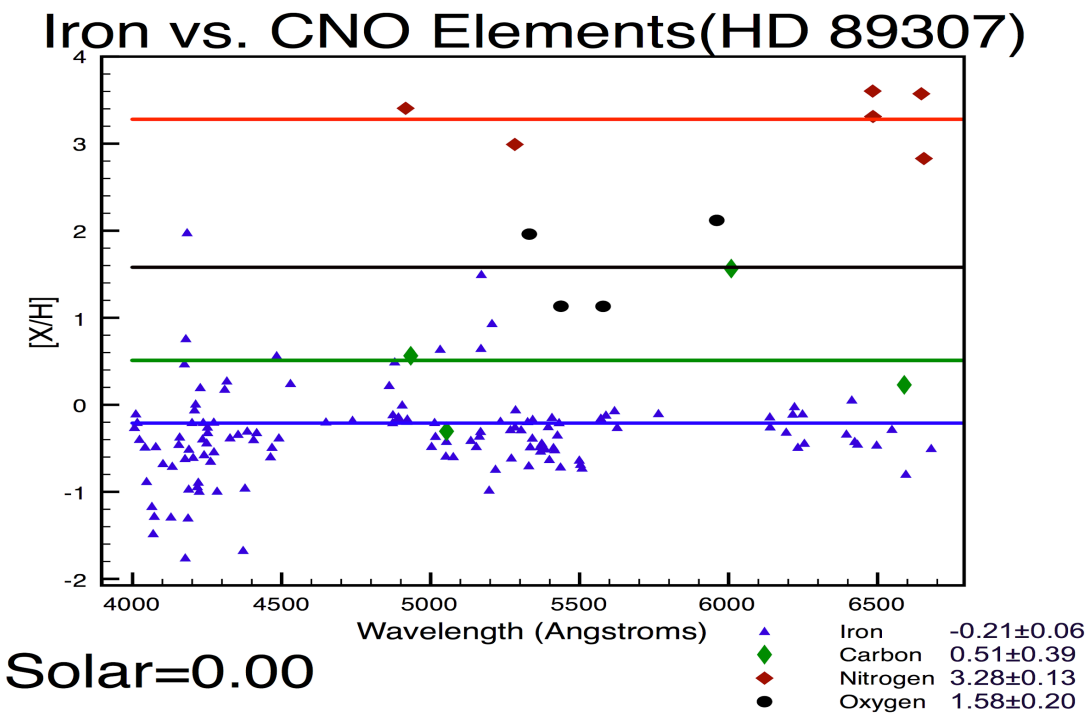
Iron vs. CNO Elements(HD 89307)
[X/H]
Wavelength (Angstroms)
Solar=0.00
Iron -0.21±0.06
Carbon 0.51±0.39
Nitrogen 3.28±0.13
Oxygen 1.58±0.20

B)

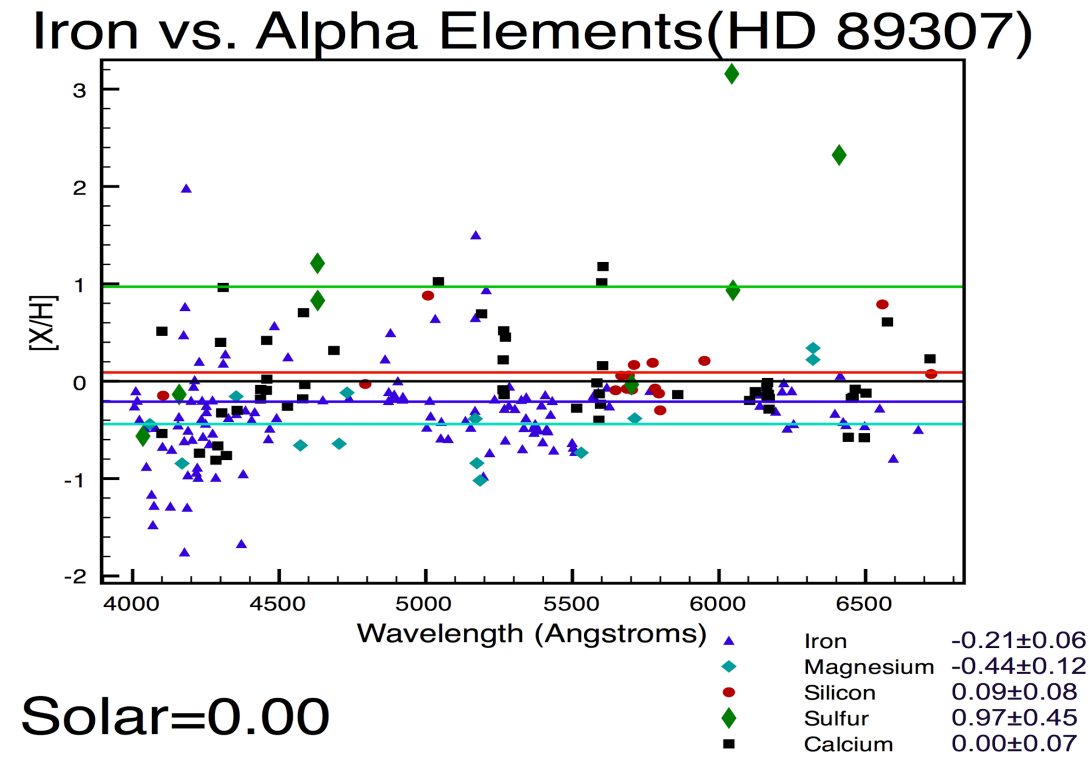
Iron vs. Alpha Elements(HD 89307)
[X/H]
Wavelength (Angstroms)
Solar=0.00
Iron -0.21±0.06
Magnesium -0.44±0.12
Silicon 0.09±0.08
Sulfur 0.97±0.45
Calcium 0.00±0.07

C)

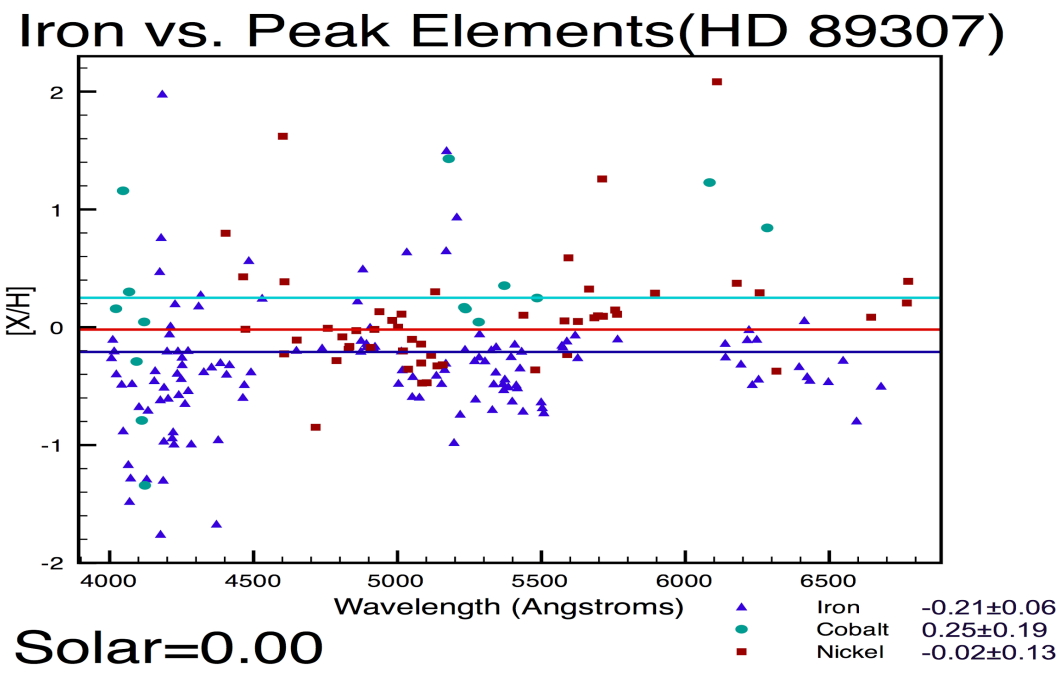

D)

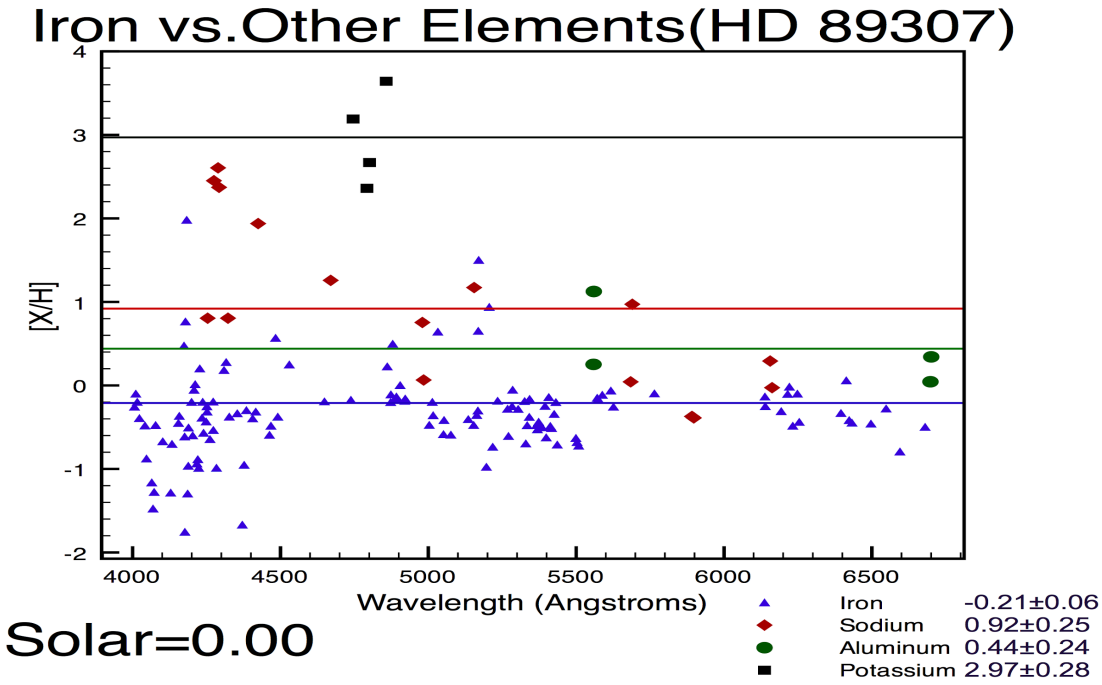

Figure 10(A-D): The results of photospheric elemental abundances of HD 89307, with iron plotted against the other element groups: CNO, iron peak elements, alpha elements, and biologically significant elements. The solid color lines represent the mean for the elemental abundance (compared to solar), which is given in the legend.

Gliese 581:

Gliese 581 was a bit more difficult to get proper equivalent width readings due to resolution issues, especially on wavelengths under 5000 Angstroms. Because of this, analysis of the absorption lines was limited to 5000-6800 Angstroms. Also, such elements as nitrogen, oxygen, potassium, carbon, and sulfur were too difficult to distinguish from the noise, and so these elements were excluded because of the lack of reliable absorption lines. Doing both a Blackwell diagram (Figure 11) for the microturbulent velocity and the normal abundance calculations (Figure 12), the iron abundance falls within the acceptable range of previously measured values (Bean, et. al., 2008). Overall, the abundance of iron, calcium and sodium seemed to follow my assumptions by being somewhat lower than solar. Nickel, cobalt, and silicon surprised me however, by being quite a bit more abundant than the given solar values.

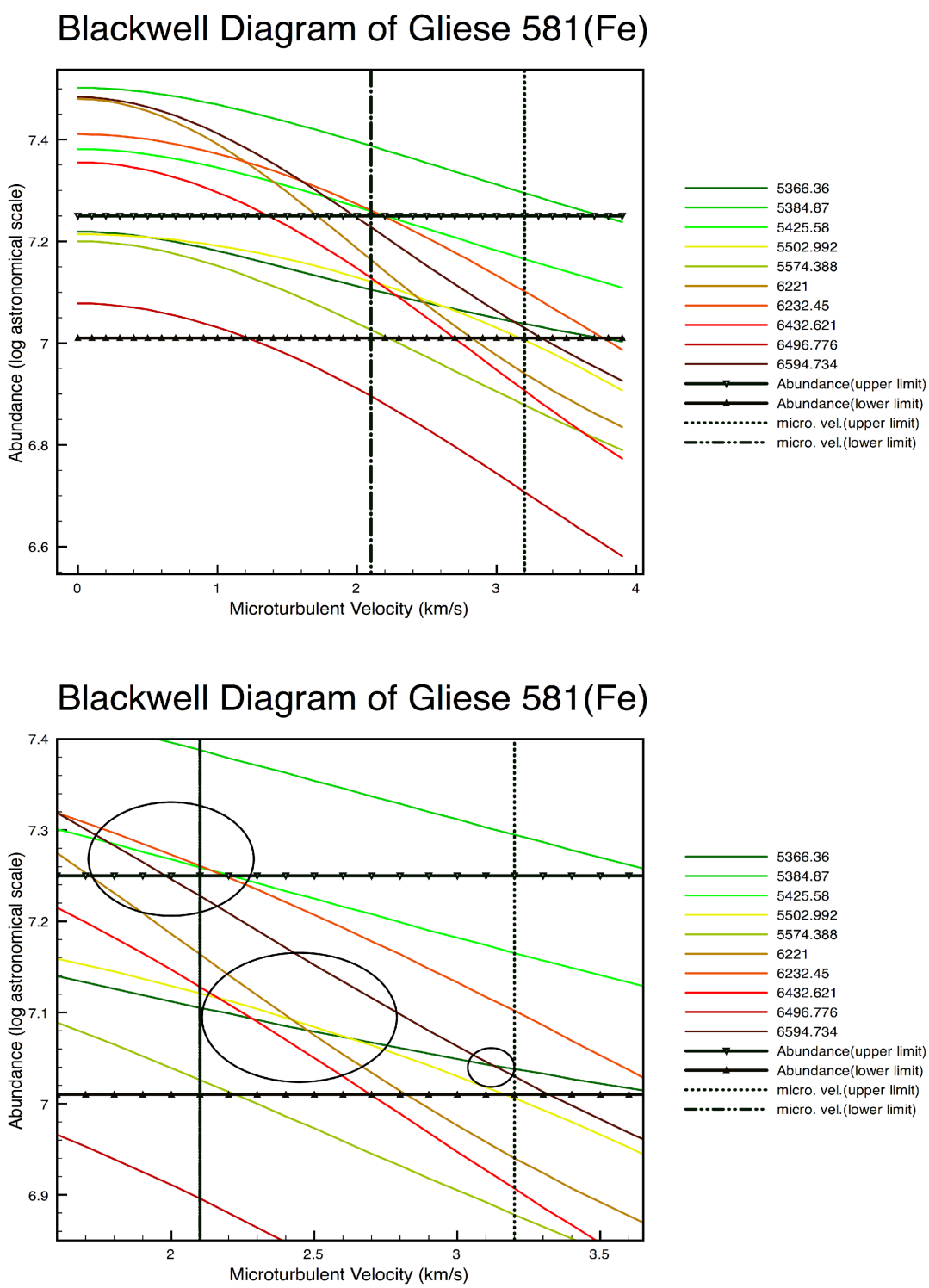

Figure 11: A Blackwell diagram (and zoomed in cut out) for Gliese 581 showing the elemental abundance of iron versus the microturbulent velocity. The observations seem to fit within the values measured by Bean, et. al., (2008). The microturbulent velocity ranges from 2.1 to 3.2 km/s.

A)

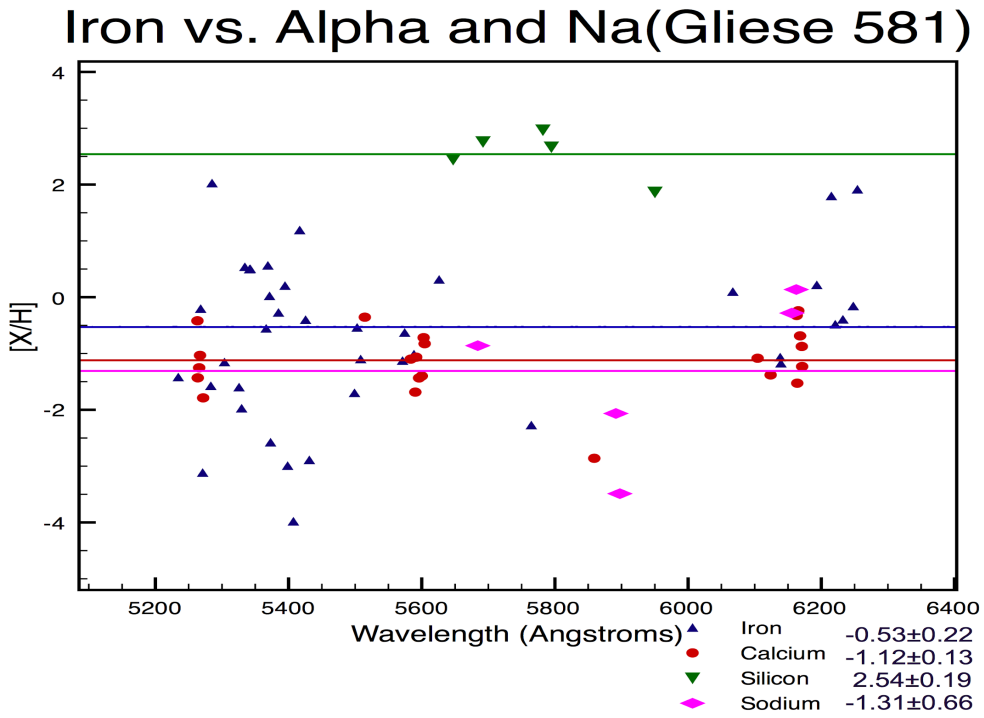

B)

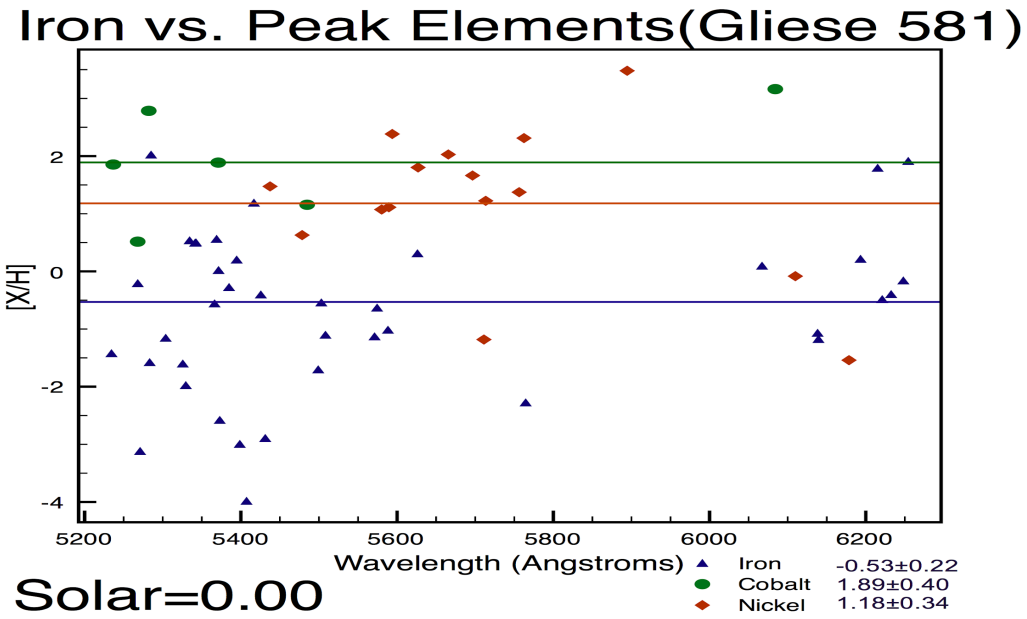

` **Figure 12(A-B): The results of the elemental abundances of Gliese 581, iron being compared to the iron peak elements, alpha elements, and sodium. Solid color lines represent the mean for each element in question.**

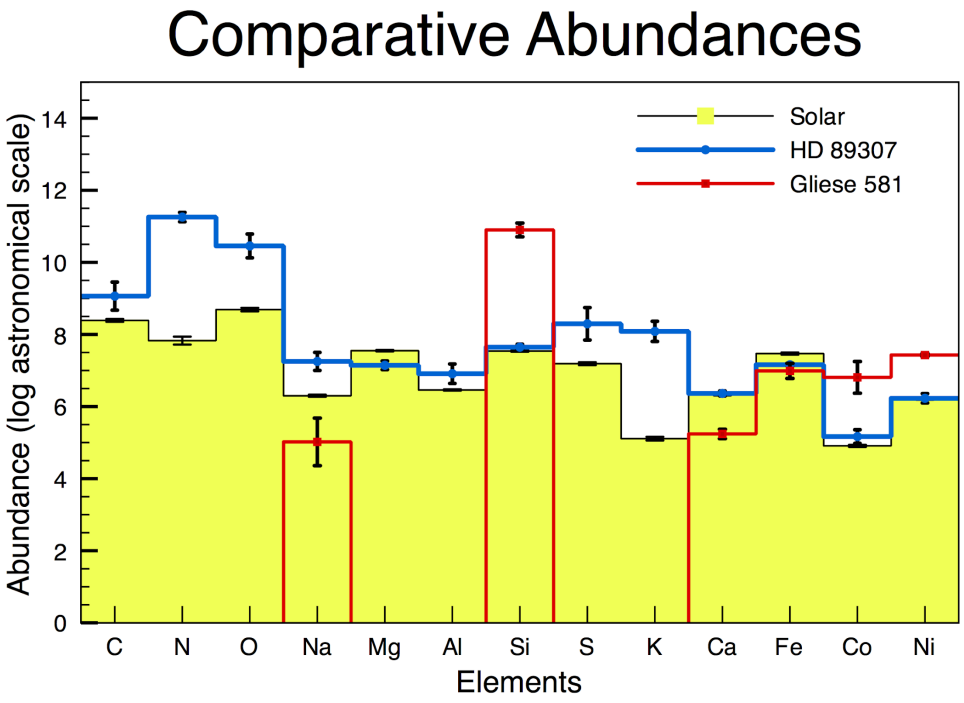

Figure 13: The abundances of the two star systems are presented along with the solar values. It would seem from the observations that there are variances amongst the elemental abundances, which warrants further study.

Comparative Results:

By comparing the sun to HD 89307 and Gliese 581, we can see some similarities, but also some distinct differences. In Figure 13, we can see the elemental abundances for each atomic species for each of the star systems in question. While Figure 13 shows that Gliese 581 has no values for certain elements, it does not mean that there is no abundance, merely that there was no good observations available for those particular absorption lines. Gliese581 presents lower values than the sun for three of the elements, but has three in particular that seem to be more abundant than solar. HD89307 seems fairly similar to solar, which is what I had expected.

Conclusion/Discussion:

Throughout this research project, the primary goal has been to gain understanding and knowledge about stellar spectra, and relative photospheric elemental abundances. Being able to replicate previously measured iron abundance for the star systems increased my confidence in my measurements. Certain abundances seemed to follow my assumptions based off of total solar system abundance values, while others did not seem to fit my expectations. When comparing iron to other element groups (CNO, alpha, iron peak, and biologically significant elements), I was able to visualize trends that could lead to better understanding of elemental formation (due to Type Ia and Type II supernovae), extrasolar system formation, and cosmochronology. With more research on other planetary systems and their host stars, there would be more information that could be learned that will help with our understanding of the formation of our solar system, as well as the formation of other planetary systems. Overall, I accomplished the goals I had set out, and performed research that is of personal interest.

To extend this study, I would alter how I made my observations and calculations. First, I would explore multiple spectra of a single star, to come up with more statistical results. I would also explore a multitude of different star systems, in order to see trends that will increase the understanding of exoplanetary star systems and cosmochronology. Instead of using a prepackaged computer program, I would instead utilize a coding language such as IDL (Interactive Data Language) to measure and visualize observational spectra. In time I believe this project could turn into a possible masters thesis, with a thorough examination of spectra coupled with careful calculations of abundances.

Acknowledgements:

I would especially like to thank my Watkins Mentor, Dr. James Jacobs for giving me the opportunity to work on an independent project in astronomy. I would also like to thank the following: Dr. Dan Reisenfeld for being my academic advisor and a great teacher; Dr. Michael Schneider who helped answer my optics questions; and Dr. Nate McCrady, my current research advisor, who has reinforced my knowledge and taught me the ins and outs of research astronomy. Special thanks go to Dr. Richard Gray, the writer of the SPECTRUM, ABUNDANCE, and BLACKWEL who answered all my emails concerning the programs and helped me troubleshoot; to Dr. Robert Kurucz for insight into his ATLAS9 models; and Dr. Peter Draper for providing his program, SPLAT-VO. I would also like to thank the ELODIE archive for making spectra available to the public. Heartfelt thanks go to Diane Friend and the late Dr. David Friend, both of whom gave me a taste of what it means to have true passion for astronomy, and if it weren't for them, I would still be a history major.

References:

Bean, J.L., Benedict, G.F., Endl, M., *Metallicities of M Dwarf Planet Hosts From Spectral Synthesis,* The Astrophysical Journal, Vol. 653, 2006

California Planet Search, The University of California, http://exoplanets.org/

Carroll, B., Ostlie, D., *An Introduction to Modern Astrophysics,* Addison-Wesley Publishing, 1996

Draper, Peter W., *Starlink SPLAT_VO,* http://star-www.dur.ac.uk/~pdraper/splat/splat-vo/

ELODIE Archive, Observatoire de Haute-Provence (OHP), http://atlas.obs-hp.fr/elodie/

Hartmann, William K., *Moons and Planets,* Brooks/Cole, 2005
Fischer, D., Driscoll, P., Isaacson, H., Giguere, M., Marcy, G., Valenti, J., Wright, J.T., Henry, G.W., Johnson, J.A., Howard, A., Peek, K., McCarthy, C., *Five Planets and an Independent Confirmation of HD196885Ab From Lick Observatory,* The Astrophysical Journal, Vol. 703, 2009

Gray, Richard, *SPECTRUM: A Stellar Spectral Synthesis Program,* http://www1.appstate.edu/dept/physics/spectrum/spectrum.html, 2008

Lodders, Katharina, *Solar System Abundances and Condensation Temeratures of the Elements,* The Astrophysical Journal, Vol.591, 2003

Kurucz, Robert L., *Grids of Model Atmospheres,* http://kurucz.harvard.edu/, 2008

Marcy, G., Butler, R.P., Fischer, D., Vogt, S., Wright, J.T., Tinney, C.G., Jones, H.R.A., *Observed Properties of Exoplanets: Masses, Orbits, and Metallicities,* Progress of Theoretical Physics Supplement No. 158, 2005

NIST: Atomic Spectra Database, http://physics.nist.gov/PhysRefData/ASD/lines_form.html